

Surface-based Transport Model for Mixed-Size Sediment

Peter R. Wilcock, M.ASCE,¹ and Joanna C. Crowe²

Abstract: We present a transport model for mixed sand/gravel sediments. Fractional transport rates are referenced to the size distribution of the bed surface, rather than subsurface, making the model completely explicit and capable of predicting transient conditions. The model is developed using a new data set of 48 coupled observations of flow, transport, and bed surface grain size using five different sediments. The model incorporates a hiding function that resolves discrepancies observed among earlier hiding functions. The model uses the full size distribution of the bed surface, including sand, and incorporates a nonlinear effect of sand content on gravel transport rate not included in previous models. The model shares some common elements with two previous surface-based transport models, but differs in using the full surface size distribution and in that it is directly developed from a relatively comprehensive data set with unambiguous measurement of surface grain size over a range of flow, transport rate, and sediments.

DOI: 10.1061/(ASCE)0733-9429(2003)129:2(120)

CE Database keywords: Sediment transport; Models; Sand; Gravel.

Introduction

The transport of sediment from a bed of mixed sizes depends on the quantity of each grain size present on the bed surface. In a gravel-bed river, the bed is often sorted such that the surface composition is coarser than the substrate. Taken together, these observations define a problem for the prediction of transport rate that has not been completely solved, because nearly all mixed-size transport formulas have been developed relative to the grain size of the substrate or bulk sediment, rather than the bed surface. A transport model referenced to the substrate grain size contains an implicit dependence on the surface sorting that determines the grains available for transport. Because surface sorting depends on factors not included in a transport model (e.g., prior flow and transport rates, mechanisms of vertical sorting), a substrate-based transport model is clearly incomplete. Unaccounted variation in the surface grain size will lead to error in the predicted transport rate.

It is commonly advised that transport models be applied only under conditions similar to those for which the model was developed. For mixed-size sediment, similar conditions are defined in terms of sediment size distribution and the intensity of the transport rate (for example, the well-known Meyer-Peter and Müller formula is often recommended for low to moderate transport rates of gravel). In the case of substrate-based transport models, it might be hoped (without explicit justification) that similar grain size and transport intensity will be correlated with similar surface sorting and, therefore, similar transport rates. This is neither a satisfying nor general solution, however, because the surface

grain size interacts not only with the flow and transport rate, but also depends on the history of water and sediment supply, factors which are not included in a transport model. More fundamentally, the underlying transport mechanism, although complex in its local detail, is a relatively simple and evidently general relation linking fluid forces and grain motions. We know of no reason why a properly formulated governing relation between fluid force and sediment reaction should not apply under the full range of conditions. It is when the problem is ill posed, as when predicting transport from bulk grain size, that uncontrolled variation in the relevant initial and boundary conditions imposes unpredictable variability in transport rate.

Beyond general theoretical considerations, a compelling reason for a surface-based transport model is that it predicts instantaneous transport rates, independent of initial and boundary conditions, and is thereby capable of predicting transient conditions. Stream beds are not typically in a steady state relative to the contemporary water and sediment supply. The rate and direction of bed adjustments and the accompanying transport rates must be predicted as a function of the composition of the changing bed surface.

The primary barrier to the development of a comprehensive surface-based transport model has been the lack of sufficient coupled observations of flow, transport, and surface grain size to develop such a relation. In the field, observations of bed surface composition are generally made during low flow, when the bed is inactive. We know of only one surface observation during active transport (Andrews and Erman 1986). There are some coupled surface/transport observations from laboratory flumes, where it is possible to shut the transport off almost instantaneously, such that the bed surface associated with a particular transport rate can be measured. The number of these observations is relatively small and most surface samples have been collected by applying an adhesive to the bed surface (e.g., Parker et al. 1982a; Proffitt and Sutherland 1983; Kuhnle 1989). Correction of sampling bias relative to the size basis used for the transport has been controversial (e.g., Ettema 1984; Church et al. 1987; Diplas and Sutherland 1988; Fripp and Diplas 1993). Further, an adhesive sample of the bed surface will tend to include both surface and subsurface grains and the distribution of subsurface grains included is likely

¹Professor, Dept. of Geography and Environmental Engineering, Johns Hopkins Univ., Baltimore, MD 21218. E-mail: wilcock@jhu.edu

²Graduate Student, Dept. of Geography and Environmental Engineering, Johns Hopkins Univ., Baltimore, MD 21218.

Note. Discussion open until July 1, 2003. Separate discussions must be submitted for individual papers. To extend the closing date by one month, a written request must be filed with the ASCE Managing Editor. The manuscript for this paper was submitted for review and possible publication on July 30, 2001; approved on October 1, 2002. This paper is part of the *Journal of Hydraulic Engineering*, Vol. 129, No. 2, February 1, 2003. ©ASCE, ISSN 0733-9429/2003/2-120-128/\$18.00.

to be size selective (Diplas and Fripp 1992; Marion and Fracarro 1997). A superior alternative uses point counting techniques, which produces a sample that is equivalent to that used to describe the transport and which unambiguously samples the surface only (Kellerhals and Bray 1971; Wilcock and McArde 1993).

In this paper, we develop a surface-based transport model for mixed sand and gravel. The model incorporates concepts found in earlier, substrate-based transport models: A hiding function (Einstein 1950; Egiazaroff 1965; Andrews and Parker 1987) and a similarity collapse over grain size based on a reference shear stress (Ashida and Michue 1971; Parker et al. 1982b). Development of the model is made possible by the availability of a new data set consisting of 48 coupled observations of flow, transport, and bed surface grain size using five different sediments in a laboratory flume (Wilcock et al. 2001).

Flume Type and Transport Models

The distinction between surface- and subsurface-based transport becomes particularly clear in the case of flume experiments. Inasmuch as most transport models are based largely or entirely on flume experiments, a clear description of this distinction becomes particularly important. Sediment is typically introduced into a flume in one of two ways. It may be fed at a specified rate or the sediment transported out of the flume can be recirculated to the upstream end. Although the equilibrium relations among discharge, transport rate, and hydraulics are identical for either flume type when using unisize sediment, the equilibrium state for mixed-size sediment can differ substantially between the two cases (Parker and Wilcock 1993).

Consider a thought experiment using a widely graded mixed-size sediment in a flume that may be operated in either feed or recirculating mode. For the recirculating case, a flow is imposed that produces an active, but moderate transport rate. We may expect that the grain size of the transport will be finer than that of the bulk mix (the difference between transport and bed grain size decreases with increasing flow and transport rate; Wilcock and McArde 1993; Wilcock 2001). Now, using the same flow and transport rate, flume operation is changed from recirculating to feed. The grain size of the feed sediment must be specified. If the feed grain size is identical to that of the transport in the first experiment, the same equilibrium conditions will be maintained. If, however, the feed grain size is identical to that of the bed (as is typically the case in feed experiments), the system will reach a new equilibrium. The bed slope will be somewhat larger and the bed surface will be coarser because the same discharge must now carry a relatively coarser transport, which is accomplished primarily by increasing the number of coarse grains on the bed surface (Parker and Klingeman 1982).

If the results of these two flume experiments were used to develop a transport model referenced to the bulk composition of the sediment, an important discrepancy becomes apparent. The transport rate is the same in both cases, as is the water discharge, but the transport grain size is different. Part of the difference between the two cases may be accounted for by a larger bed stress in the feed case, but the primary reason for the difference in transport, the difference in bed surface composition, is not included in the model. The model is incomplete: The same bed size distribution is associated with more than one transport size distribution. By referencing the transport rates to the bed surface composition, the differences between the two runs are completely described. The two cases represent different equilibrium conditions corresponding to different boundary conditions; the flow/

bed/transport interaction in each case is represented by the bed stress, transport rate, and grain size of the transport and bed surface. A general transport model requires all these elements. Empirical transport models based on bulk or substrate grain size contain an implicit relation between substrate and surface grain size distributions and should be used with caution.

Previous Models

Two previous surface-based transport models have been defined. Proffitt and Sutherland (1983) developed a model based on the armoring experiments of Proffitt (1980), which included molten-wax measurements of the bed surface before and after armoring runs with four mixed sand/gravel sediments. Parker (1990) developed a model based on the well-known Oak Creek data of Milhous (1973). In this case, only a single bed surface size distribution was available, leading Parker to transform a substrate-based transport model using the available surface size distribution. A limitation of the Oak Creek model is that it is defined relative to only those sizes coarser than 2 mm. Wilcock et al. (2001) have demonstrated that the bed sand content has an important and non-linear effect on gravel transport rate; this effect cannot be captured in the Oak Creek model. A summary of both earlier surface-based transport models is given by Parker and Sutherland (1990). The transport model developed here will be compared to these two models in a later section.

Surface-based Transport Observations

The transport model is developed from coupled observations of flow, transport, and bed surface grain size in a laboratory flume. The methods used and an analysis of the results are described by Wilcock et al. (2001) and are summarized here. The entire data set may be downloaded from an archival web site. [Available via Web browser or via Anonymous FTP from ftp://agu.org, directory "append" (Username="anonymous", Password="guest"); sub-directories in the ftp site are arranged by paper number; data in paper number 2001WR000683. Information on searching is found at http://www.agu.org/pubs/esupp_about.html.] Five experimental sediments were prepared by adding different amounts of sand to a gravel mixture (Fig. 1). The gravel ranged in size from 2.0 to 64 mm, the sand from 0.5 to 2.0 mm. The proportion of sand in the mixture was varied from 6.2 to 34.3%. Four of the sediments were named according to the target sand content such that the sediment name and actual sand content were J06 (6.2%), J14 (14.9%), J21 (20.6%), and J27 (27%). These sediment mixtures were drawn from a previously used sediment BOMC (Bed of Many Colors; Wilcock and McArde 1993) which contained 34.3% sand. About one half of the sand in BOMC is in the range of 0.21 to 0.5 mm, making its sand size approximately half that of the present series (Fig. 1).

We use observations from nine or ten experimental runs with each sediment. Flow depth was held within a narrow range for all flume runs, with a minimum 0.09 m and a maximum 0.12 m and 85% of the runs between 0.10 and 0.11 m. Transport rates with each mixture varied over at least four orders of magnitude with a minimum of at most $1.8 \times 10^{-5} \text{ kg m}^{-1} \text{ s}^{-1}$ and a maximum of at least $1.2 \times 10^{-1} \text{ kg m}^{-1} \text{ s}^{-1}$. Transport of the coarsest grains occurred exclusively as bed load, as was the case for the finer (sand) fractions at small transport rates. At larger transport rates, a portion of the sand followed low trajectories that rarely exceeded the elevation of the tops of the coarser gravel clasts on the bed surface. Although portions of the sand trajectories were likely influ-

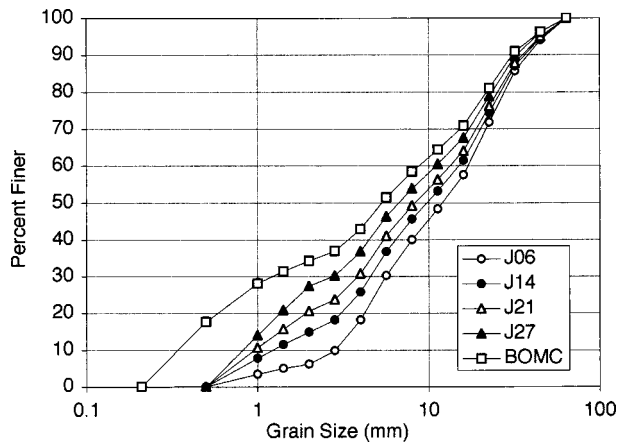


Fig. 1. Grain-size distribution of sediments used in flume experiments

enced by turbulence, we find that any distinction between bed load and suspended load is neither apparent nor useful for a complex, mixed-size transport field of medium to coarse sand and gravel and we find the term “bed material load” to be more appropriate.

The experiments were conducted in a tilting laboratory flume (dimensions of the working section are 0.6 m cross stream by 8.0 m down stream) in which both water and sediment were recirculated. Grains coarser than 16 mm were recirculated manually, which allowed nearly continuous sampling throughout a run. The total transport rates of the finer fractions were sampled volumetrically with a rapid return to the flume and samples collected at the end of the run were used to determine grain size. These samples can be correlated with the bed surface remaining at the end of the run. Sample duration was limited to avoid interfering with the flow/bed/transport interaction in the sediment recirculating flume, producing some scatter in the measured transport rates. Scatter in total transport rates, which were sampled volumetrically with immediate return (allowing a longer sample period) is smaller than for fractional transport rates, which required removing a small amount of transported sediment from the system for sieving. Some scatter in the transport rates for the coarser grains can also be attributed to the very small transport rates in some runs, with a sample sometimes consisting of only a few grains over the course of a run. Fractional transport rates are calculated as $q_{bi} = (p_i)q_b$, where p_i is the proportion of each fraction in transport and q_b is the total transport rate.

A suite of hydraulic measurements were made during each run, including water discharge, surface velocity, and the elevation of the water and bed surface along the flume. The bed shear stress was corrected for sidewall effects, following the method of Vanoni and Brooks (1957), as modified by Chiew and Parker (1994). Transport samples were collected for steady-state conditions defined by a stable mean in transport rate and size distribution.

Each grain size in the sediment was painted a different color (Wilcock and McArdell 1993). Standard $1/2\phi$ fractions were used to define all size fractions coarser than 1 mm; grains in the 0.5–1.0 mm range were grouped into one fraction. The grain-size distribution of the bed surface was measured by projecting photographs of the bed onto a grid and tallying the grain color (hence, size) falling on the grid intersections. Each photograph covered a 0.20×0.27 m bed section such that two adjacent photographs provided continuous cross-stream coverage of 40 cm. Individual

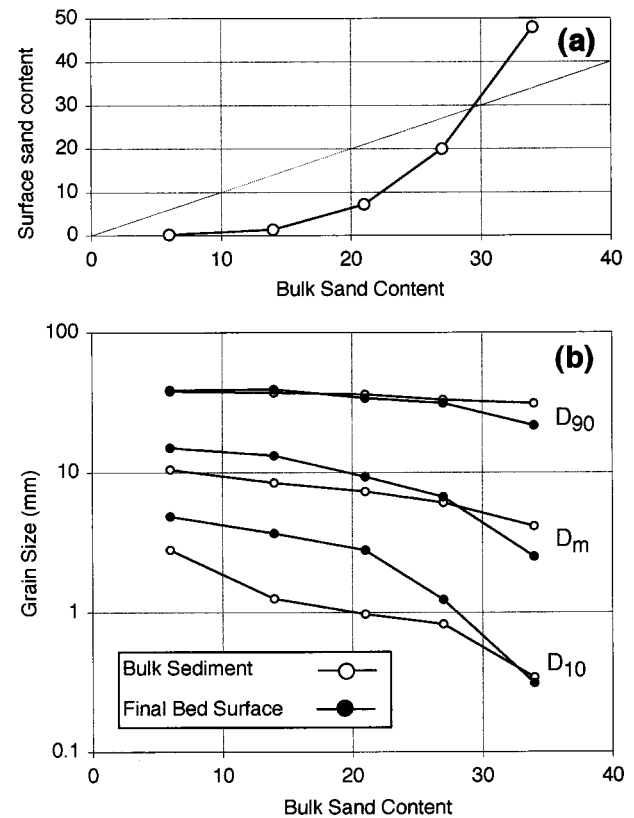


Fig. 2. Surface grain size as a function of bulk sediment sand content. (a) Mean surface sand content F_s . (b) Mean surface grain size D_{sm} , along with 10th and 90th percentiles. Also shown are equivalent percentiles for bulk sediment.

grains were identifiable for all fractions. The remaining 10 cm on each side of the flume was not photographed. Point counts were conducted for the down stream 4 m of the flume and a point count typically consisted of 3,920 points (c.f., Rice and Church 1996). This large number of points was used in order to estimate the proportion F_i of each size fraction on the bed surface. The grid-by-number method used here to determine the bed surface grain-size distribution has been shown to be equivalent to the volume-by-weight method commonly used in bulk sampling and sieve analyses (Kellerhals and Bray 1971; Church et al. 1987). Based on a previous analysis of replicate point counts and a comparison between bulk and screeded beds, we suggest that a conservative estimate of the error in measuring F_i is $\pm 30\%$ (e.g., for an observed $F_i = 0.1$, the true value is likely to fall within 0.07 and 0.13). The actual error in most cases should be considerably smaller (Wilcock and McArdell 1993).

Bed Adjustments

The transport model developed here is defined relative to the size distribution of grains available for transport on the bed surface. Some description of the surface composition observed during the runs helps to interpret the transport rates we model. Fig. 2 summarizes the principal adjustments of the bed surface over the course of the flume runs. In general, the variation of the bed surface from run to run was much smaller than the variation from sediment to sediment (Wilcock et al. 2001). The values given in Fig. 2 are averages for the bed surface at the end of all runs with a particular sediment. For all but the sandiest sediment (BOMC),

the sand content of the bed surface was smaller than that of the bulk sediment and substrate [Fig. 2(a)]. The reduction in sand content for the least sandy sediments, J06 and J14, was particularly important, with final surface sand contents of 0.1 and 1.3%, respectively. In these cases, nearly all of the sand initially on the bed surface worked its way into the subsurface over the course of the run (Wilcock and Southard 1989; Parker and Wilcock 1993). This reduction of fines content on the bed surface is also evident in percentile values of grain size [Fig. 2(b)]. Values of D_{90} (90% of the size distribution finer) are relatively stable over all sediments, whereas D_{10} shows an increase in grain size from bulk to surface for all sediments except the sandiest. The median surface size D_{50} shows a coarsening for the least sandy sediments and a fining for the sandiest sediment [Fig. 2(b)], an observation that will have direct bearing on the transport model developed here.

The Model

The transport model is developed using a similarity collapse over fractional transport rate, as used successfully for substrate-based empirical models (e.g., Ashida and Michue 1971; Parker et al. 1982b). The form of the similarity collapse is

$$W_i^* = f(\tau/\tau_{ri}) \quad (1)$$

where τ =bed shear stress, τ_{ri} (the similarity parameter) =reference value of τ , and W_i^* =defined by

$$W_i^* = \frac{(s-1)gq_{bi}}{F_i u_*^3} \quad (2)$$

where s =ratio of sediment to water density; g =gravity; q_{bi} =volumetric transport rate per unit width of size i ; F_i =proportion of size i on the bed surface; and u_* =shear velocity ($u_* = [\tau/\rho]^{0.5}$); and ρ =water density.

Reference Shear Stress

The reference shear stress τ_{ri} is defined as the value of τ at which W_i^* is equal to a small reference value $W_r^* = 0.002$ (Parker et al. 1982a,b; Wilcock 1988). Values of τ_{ri} were determined by eye on plots of scaled fractional transport rate q_{bi}/F_i for each fraction. In 47 of the 64 cases, fractional transport observations extended both above and below W_r^* and τ_{ri} was determined by interpolation. In 11 of the remaining cases, the smallest transport observation fell within one order of magnitude of W_r^* and required minimal extrapolation. Six cases required extrapolation over more than one order of magnitude in W^* (mostly for the largest two sizes). Greatest weight in choosing τ_{ri} was given to transport observations in the vicinity of W_r^* , thereby preserving an interpretation of τ_{ri} as a surrogate for the fractional critical shear stress τ_{ci} . In cases requiring extrapolation, or where the transport data were more scattered, increased weight was given to the overall trend of the fractional transport data, in which case, a relation similar to the final transport curve was used to aid the choice of τ_{ri} . Fitting was done by eye because the procedure is multipart, involves strongly nonlinear functions, and optimized solutions for τ_{ri} tend to be strongly influenced by outliers and are, to the eye, inferior. Fitting by eye also facilitates assignment of different weights to individual data points according to the scatter in the individual trends and the need to extrapolate them to W_r^* . To provide bounds on the fitted result, the smallest and largest values of τ_{ri} that could reasonably fit the transport data were recorded and are presented here as error bars.

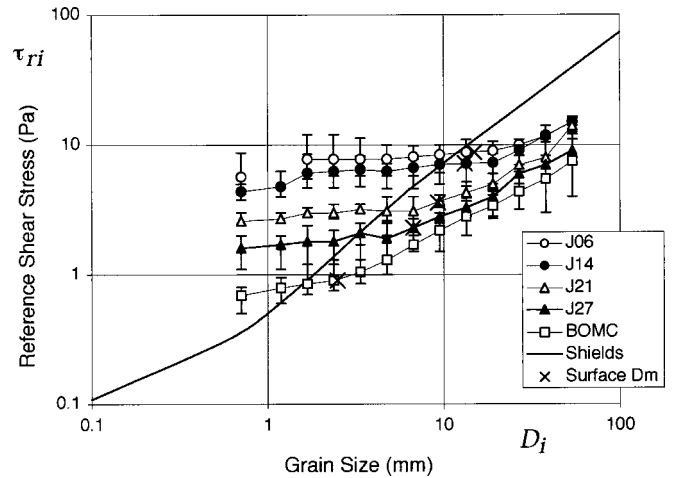


Fig. 3. Reference shear stress τ_{ri} for each size fraction. Error bars represent conservative estimate of largest and smallest value consistent with transport observations. Also shown are interpolated values at average D_{sm} for each sediment. Shields curve for unisize sediment is shown for comparison.

The fitted τ_{ri} are given in Fig. 3. Significant variation in the trends of the different mixtures is evident. The mixture with least sand (J06) shows the smallest variation of τ_{ri} with grain size (approaching grain-size independence, one element of the condition of equal mobility, Parker et al. 1982b). The variation of τ_{ri} with grain size increases with mixture sand content. The sandiest mixture (BOMC) shows a continuous increase of τ_{ri} with D_i . Values of τ_{rm} , the value of τ_{ri} corresponding to the mean size of the bed surface D_{sm} are also shown on Fig. 3. The τ_{ri} trend for each mixture shows a break in slope near D_{sm} , wherein the variation of τ_{ri} with D_i is much smaller for sizes smaller than D_{sm} .

Hiding Function

A general model for τ_{ri} requires a consistent collapse leading to a single predictive relation. Values of τ_{ri} are scaled by τ_{rm} for each mixture and plotted as a function of D_i/D_{sm} in Fig. 4. The collapse in the five trends is quite good and remarkable for the fact that a single dimensionless trend exists for mixtures with a wide range of sand content. The trend in Fig. 4 clearly has two linear segments, suggesting that it may be represented by the power function

$$\frac{\tau_{ri}}{\tau_{rs50}} = \left(\frac{D_i}{D_{s50}} \right)^b \quad (3)$$

with two values of the exponent b . Values shown in Fig. 4 are $b = 0.12$ for $D_i/D_{sm} < 1$ and $b = 0.67$ for $D_i/D_{sm} > 1$. A two-piece linear trend deviates somewhat from the data over the range $1 < D_i/D_{sm} < 3$, and a smooth variation in b provides a better fit. Also shown in Fig. 4 is Eq. (3) using the exponent

$$b = \frac{0.67}{1 + \exp\left(1.5 - \frac{D_i}{D_{sm}}\right)} \quad (4)$$

which provides a satisfactory fit to the data.

Eqs. (3) and (4) represent a hiding function analogous to that used in previous mixed-size transport models (e.g., Einstein 1950; Egiazaroff 1965; Parker et al. 1982b; Proffitt and Sutherland 1983; Andrews and Parker 1987; Sutherland 1992) in that it acts

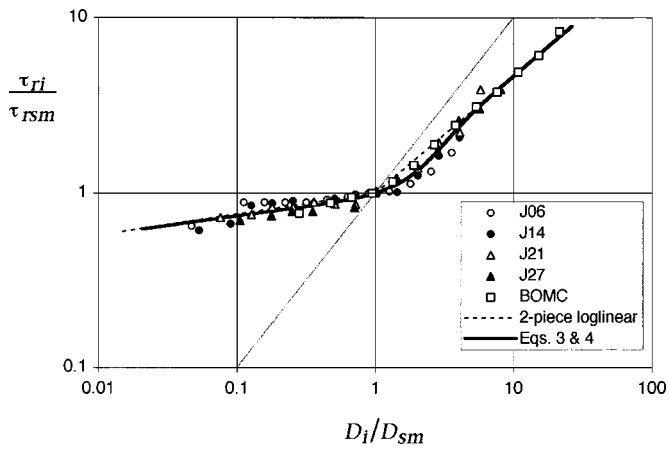


Fig. 4. Reference shear stress for each size fraction, scaled by reference shear stress for the mean of each bed surface D_{sm} , as function of fraction size D_i scaled by D_{sm} . The trend is clearly different for D_i/D_{sm} greater or smaller than one and may be fitted using Eq. (3) using two log linear segments or with continuously varying exponent [Eq. (4)].

to increase τ_{ri} (reducing calculated transport rates) for finer fractions and reduce τ_{ri} (increasing calculated transport rates) for coarser fractions, relative to values of τ_r for single-sized sediments, as indicated approximately by the 1:1 line in Fig. 4.

The two-part trend to the hiding function in Fig. 4 sheds light on an unresolved problem in modeling the incipient motion of mixed-size sediment. Some have observed that the variation of τ_{ri} with grain size tends to be relatively small, corresponding to a value of b close to 0 (e.g., Parker et al. 1982b; Andrews and Parker 1987; Wilcock and Southard 1988), whereas others have found much greater size dependence in τ_{ri} , with values of b exceeding 0.5 (Wilcock 1993; Ashworth and Ferguson 1989). Generally, small values of b have been reported for gravel beds with small fines content (e.g., Oak Creek, Parker et al. 1982b), whereas larger values of b have been reported for sandy gravels (e.g., BOMC, Wilcock 1993; Goodwin Creek, Kuhnle 1993). The trend in Fig. 4 helps to explain this difference, when coupled with our observations of the variation in D_{sm} from mixture to mixture. The mean surface grain-size D_{sm} is relatively coarse in the less sandy mixtures and much finer in the sandier mixtures [Fig. 2(b)]. This is a function not only of the overall increase of sand in the bulk mix, but also of selective sorting between surface and substrate [compare surface and bulk D_{sm} in Fig. 2(b)]. Bulk D_m decreased by a factor of 2.3 over the five mixtures, whereas D_{sm} decreased by a factor of 6.4. A sandier mixture, with a relatively small D_{sm} will have more fractions falling on the steep upper limb of the hiding function (BOMC on Fig. 4), whereas a less sandy mixture, with a relatively large D_{sm} will have more fractions falling on the gentle lower limb of the hiding function (J06 and J14 on Fig. 4).

A complete model requires a basis for predicting τ_{rm} . Values of τ_{rm} for the five experimental mixtures (determined directly from Fig. 3) are plotted as the Shields number

$$\tau_{rm}^* = \frac{\tau_{rm}}{(s-1)\rho g D_{sm}} \quad (5)$$

versus the percent sand on the bed surface F_s in Fig. 5. A smooth curve is fitted to the data

$$\tau_{rm}^* = 0.021 + 0.015 \exp[-20F_s] \quad (6)$$

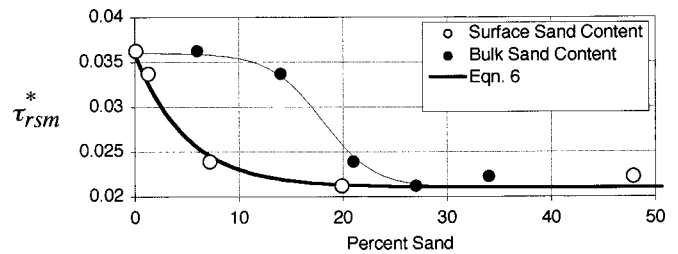


Fig. 5. Variation of Shields number for reference shear stress at D_{sm} , as function of surface sand content F_s . Also shown are same values of τ_{rm}^* plotted as function of sand content of bulk sediment.

The value of τ_{rm}^* decreases from 0.036 to 0.021 over the range in F_s . Based on an analysis of additional laboratory and field transport data (Wilcock 1998; Wilcock and Kenworthy 2002) it is likely that the trend in Fig. 5 does not decrease further at larger F_s . Also shown on Fig. 5 are the same values of τ_{rm}^* plotted against the percent sand in the bulk sediment. This trend shows that the decrease in τ_{rm}^* occurs over a range in sand content of approximately 15–25%, which corresponds to the transition from a framework-supported to a matrix-supported gravel bed, providing a physical explanation for the shift in the behavior shown in Fig. 5 (Wilcock 1998).

The reduction of τ_{rm}^* with sand content represents a significant departure between the current model and previous models in that it represents a direct and nonlinear relation between sand content and transport rate. As sand content increases, τ_{ri} for all sizes decreases through Eqs. (6) and (3), thereby increasing transport rates. This effect of sand content on transport rate was initially indicated in the work of Jackson and Beschta (1984) and Ikeda and Iseya (1988) and is clearly demonstrated by the flume results used to develop the present model, which were designed to demonstrate explicitly the effect of sand content on transport rate (Wilcock et al. 2001).

Transport Function

W_i^* is plotted as a function of τ/τ_{ri} for all size fractions and experimental runs (Fig. 6, $N=450$). Although there is some scatter in the data, the trend is clear. The function fitted to the transport observations is

$$W_i^* = \begin{cases} 0.002\phi^{7.5} & \text{for } \phi < 1.35 \\ 14 \left(1 - \frac{0.894}{\phi^{0.5}} \right)^{4.5} & \text{for } \phi \geq 1.35 \end{cases} \quad (7)$$

where $\phi = \tau/\tau_{ri}$. This function was selected to preserve some of the form of the earlier transport function of Parker (1990), including the asymptotic approach of W_i^* to a constant at large values of ϕ (Yalin 1972; Parker and Klingeman 1982).

Residuals

Residuals are calculated as the ratio of predicted to observed W_i^* for all fractions and all runs [Fig. 7(a)]. There is some underprediction at the smallest τ/τ_{ri} and the median and mean residuals are 1.2, indicating some bias, which occurs primarily over the range $1 < \tau/\tau_{ri} < 3$. 56% of the residuals fall within a factor of two of unity and 87% fall within a factor of five. Some of the scatter in the predictions can be attributed to the relatively short transport samples collected during the flume run, in order to minimize in-

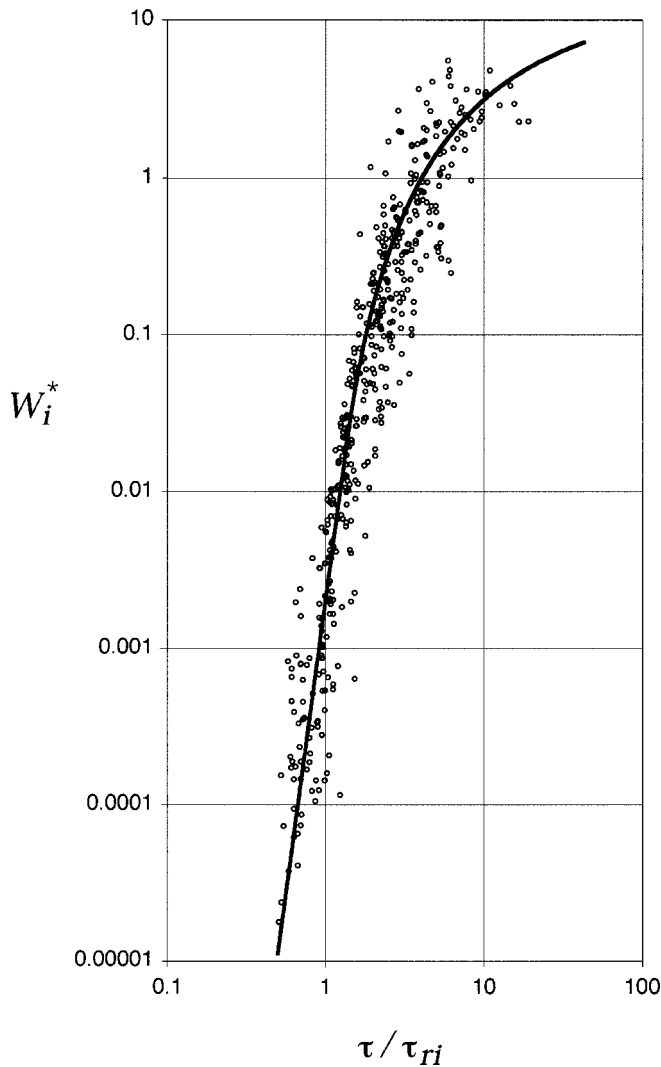


Fig. 6. Similarity collapse of all fractional transport observations

terruption of the transport system (Wilcock et al. 2001). There is little consistent bias in the residuals with grain size, although there is a slight tendency for the transport of the coarsest two fractions to be underpredicted [Fig. 7(b)].

Application

Eqs. (3), (6), and (7) define the surface-based transport model. Direct application requires specification of τ and the surface size distribution (F_i, D_i), from which the fractional transport rates are calculated. D_{sm} is determined from F_i and τ_{rm} is found from Eq. (6), using Eq. (5). Values of τ_{ri} are found from Eq. (3), using Eq. (4). Values of ϕ are calculated for each D_i and fractional transport rates are found from Eq. (7), using Eq. (2). A surface-based model can also be used in an inverse application, in which the surface size distribution (F_i, D_i) is found as a function of a specified transport rate. In this case, the transport size distribution (p_i, D_i) is specified along with either τ or the total transport rate q_b . A solution of the problem is iterative using an approach described by Parker (1990) or Parker and Wilcock (1993).

Spatial variability of surface grain size in the field presents a difficult problem for any transport calculation. The transport function depends strongly on grain size through the hiding function and is strongly nonlinear.

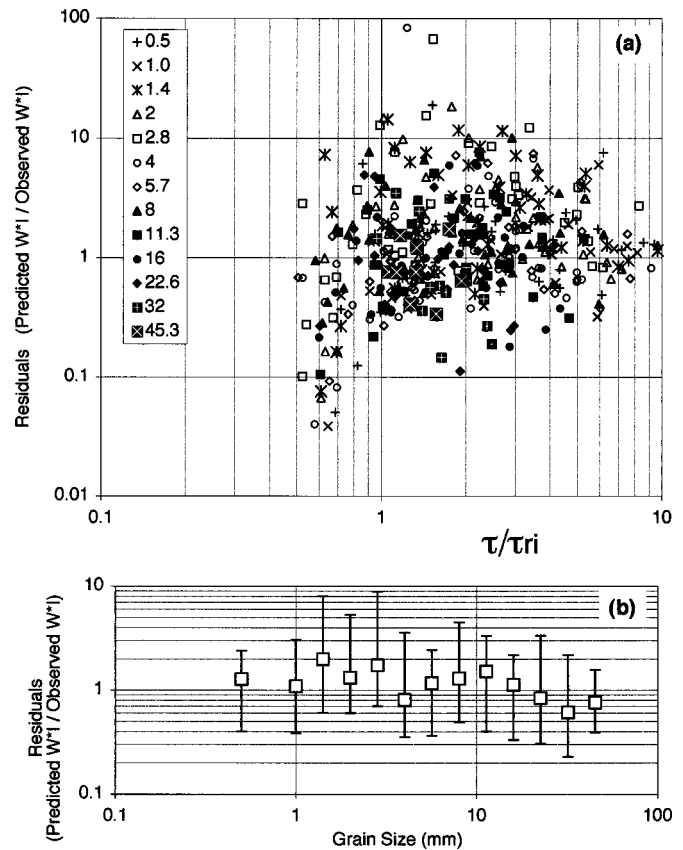


Fig. 7. Residuals between fitted model and measured transport. (a) Residuals as function of scaled shear stress, by grain size. (b) Residuals as function of grain size; square gives median residual, error bars indicate 90th and 10th percentile of residuals.

In common application, specification of F_i is a nontrivial matter. Surface grain size can be sampled at low flows, but at higher flows producing substantial transport, bed measurements are prohibitively difficult and dangerous. There is some indication that the surface grain size may vary little with increasing flows in many gravel-bed rivers (Andrews and Erman 1986; Wilcock 2001), suggesting that a surface observation at low flow may be used to approximate the bed surface at large flows. Support for this conclusion is found in the relatively small variation in surface grain size observed in the experiments used here, which covered a wide range in transport rates (Wilcock et al. 2001). These experiments were conducted in a sediment recirculating flume, for which the transport grain size increases with τ , as is typically found in gravel-bed rivers [sediment feed flumes, for which the transport grain size is typically held constant over a range of flows, provide a less realistic simulation of the adjustments of the bed surface with flow (Parker and Wilcock 1993; Wilcock 2001)]. Nonetheless, direct observation of a persistent surface grain size in the field is limited to only one observation at moderate transport intensity (Andrews and Erman 1986) and others have suggested that armor layers may become progressively finer as flow increases (e.g., Parker and Klingeman 1982).

Direct application of a surface-based transport model can be made in a computational model, for which the surface composition is a matter of specification rather than measurement. In this context, a surface-based model is particularly useful for examining scenarios of bed and channel adjustment to changes in water and sediment supply.

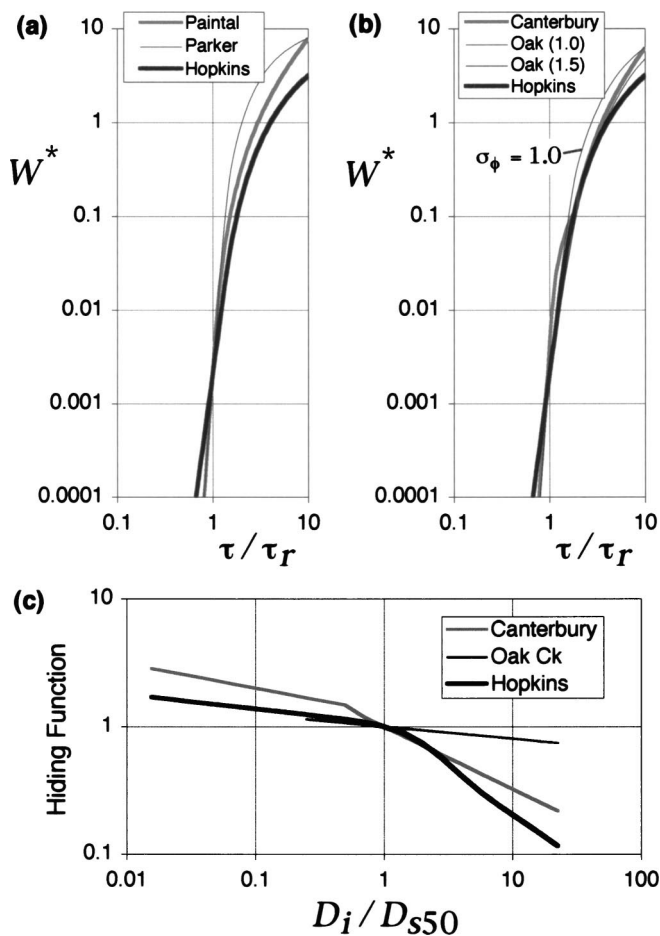


Fig. 8. Comparison of surface-based transport model to earlier models of Proffitt and Sutherland (1983; “Canterbury”) and Parker (1990; “Oak Creek”). (a) Transport functions: Paintal transport function used in Canterbury model, Parker transport function used in Oak Creek model, and Eq. (7) (“Hopkins”). (b) Same as (a), except values for Paintal function have been reduced by using parameter Δ defined by Proffitt and Sutherland (1983) and values for Oak Creek function have been reduced by using straining parameter ω , which is calculated for a phi standard deviation $\sigma_\phi = 1.0$ and $\sigma_\phi = 1.5$ (c) Hiding functions used in three models.

Comparison with Previous Transport Models

The surface-based transport model developed here is compared to the Canterbury (Proffitt and Sutherland 1983) and Oak Creek (Parker 1990) models in Fig. 8. Details about these models may be found in the original publications and a summary of both models is given in Parker and Sutherland (1990). The Canterbury model is based on the transport function of Paintal (1971), which can be expressed as a relation between W_i^* and τ/τ_{ri} if $\tau_r^* = 0.03$. Proffitt and Sutherland introduced a parameter Δ which depends on τ_{s50}^* and used $(\Delta\tau^*)$ as the argument in the Paintal model. The Paintal transport model is shown in Fig. 8(a) and corresponding values of W_i^* calculated using $(\Delta\tau^*)$ are shown in Fig. 8(b). The Oak Creek model uses a transport function nearly identical to that of Parker et al. (1982b). In developing the surface-based form of this model, Parker (1990) introduced a straining parameter ω , which depends on τ/τ_{ri} and the standard deviation σ_ϕ of the surface grain-size distribution measured in ϕ units. The Parker transport function is shown in Fig. 8(a) and

corresponding values of W_i^* calculated using $(\omega\tau/\tau_{ri})$ as the argument in the Parker relation are shown in Fig. 8(b). Two Oak Creek trends are shown, corresponding to ω calculated for $\sigma_\phi = 1.0$ and $\sigma_\phi = 1.5$, values which span the range of many gravel-bed rivers [e.g., $\sigma_\phi = 1.17$ for the surface and $\sigma_\phi = 1.5$ for the substrate of Oak Creek, when the size distribution is censored at 2 mm, as done by Parker (1990)]. It may be seen that the similarity between Eq. (7) (termed the Hopkins model) and the Paintal and Parker transport functions markedly increases when the latter transport functions are modified by the parameters introduced in the Canterbury and Oak Creek models. The Hopkins transport function contains no additional parameters and the identical trend is plotted in Figs. 8(a and b).

Proffitt and Sutherland (1983) developed a hiding function for their laboratory measurements by examining the ratio of predicted to observed transport rate. Parker (1990) developed a hiding function using a similarity collapse similar to that used here. These hiding functions are compared in Fig. 8(c) with the hiding function developed in this paper. Because each hiding function is defined somewhat differently, and the Canterbury hiding function has a weak dependence on τ^* , no single comparison among them is possible, although the relative variation in trends for different conditions are very minor. The Canterbury hiding function multiplies τ_i^* , giving larger values for small sizes and smaller values for large sizes. The Oak Creek and Hopkins hiding functions reduce τ_{ri} for smaller sizes and increase τ_{ri} for larger sizes. For comparability, the inverse of the Oak Creek and Hopkins hiding functions are plotted in Fig. 8(c). All three are plotted as the ratio of the hiding function for each fraction, divided by its value at D_{sm} . The Oak Creek hiding function has a limited extent for finer sizes, a result of censoring sand from the size distribution.

Both the Canterbury and Hopkins hiding functions show a stronger variation with relative grain size than the Oak Creek model [Fig. 8(c)], particularly for sizes coarser than D_{sm} . The Canterbury and Hopkins functions are both based on surface observations for a range of transport conditions, whereas the Oak Creek hiding function is developed from a single surface size distribution, suggesting that the different trends for relatively fine and coarse grains are real. The Hopkins hiding function has similar values to the Oak Creek hiding function for smaller sizes and the Hopkins hiding function shows a similar, but steeper, decrease at larger sizes relative to the Canterbury hiding function.

Representative transport calculations using the three models are shown in Fig. 9 for a mixed-size sediment with $F_s = 0.15$ and an approximately uniform distribution between 2.83 and 64 mm. Calculations are made with and without sand for the Canterbury and Hopkins model, to allow direct comparison with the Oak Creek Model. Transport is plotted as the scaled fractional transport rate q_{bi}/F_i as a function of D_i , which provides a clear illustration of the differences in calculated transport rates (Wilcock and Southard 1989). Differences between the calculated transport rates are greatest at small values of τ_{sm}^* , where transport rates for the coarse fractions drop off rapidly in the Canterbury and Hopkins models. In the Oak Creek model, the decrease in transport rate with D_i is constant for all sizes and is similar to the Canterbury and Hopkins models only for finer sizes. The Hopkins and Canterbury models give similar transport rates in this illustration, although for other sediments, the Canterbury model predicts larger transport rates. For the finer fractions, the without-sand estimates for the Hopkins model fall closer to the Oak Creek values and the Canterbury model gives considerably larger transport. Calculations with sand tend to produce a substantial increase

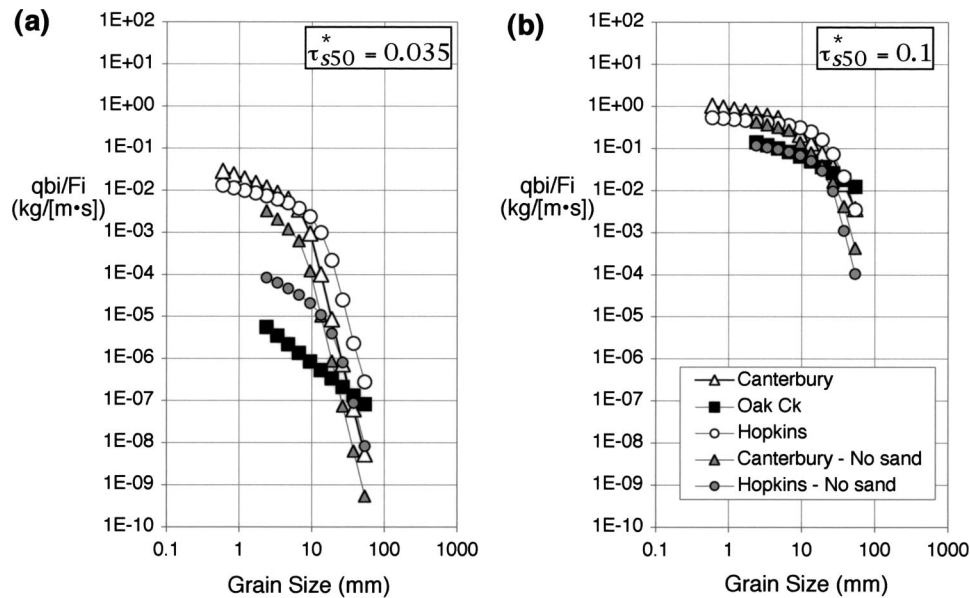


Fig. 9. Example calculations using three surface-based transport models. Sediment used has surface size distribution with 15% sand and approximately uniform size distribution between 2.83 and 64 mm. Calculations with Canterbury and Hopkins models are made with and without sand. (a) τ specified to give $\tau_{sm}^* = 0.035$. (b) τ specified to give $\tau_{sm}^* = 0.1$.

in the transport rate of finer grains, particularly for the Hopkins model, a result of the dependence of τ_{sm}^* on F_s . The calculated transport rates tend to converge to a common trend as τ_{sm}^* increases [Fig. 9(b)]. The Hopkins and Canterbury models produce much stronger selective transport of the finer half of the surface size distribution and larger transport rates, particularly at smaller τ_{sm}^* and for sediments with larger F_s .

Conclusions

The transport produced from a bed of mixed grain sizes depends on the population of grains immediately available on the bed surface. A correctly formulated and completely explicit transport model must be referenced to the bed surface; substrate models include an undefined implicit dependence on the surface sorting, which is contingent on the history of water and sediment supply. A surface-based transport model is capable of predicting transient conditions of bed armoring, scour, or aggradation.

We present here a surface-based transport model for mixed sand/gravel sediments. Model development is made possible by the availability of a new data set giving coupled observations of flow, transport, and surface grain size in 48 flume runs using five different sand/gravel sediment mixtures. This is the first relatively comprehensive record of surface-based transport observations with an unambiguous measurement of surface grain size for a range of sediment, flow, and transport rate. The model uses the full size distribution of the bed, unlike a previous model that requires the surface size distribution to be censored at 2 mm. Incorporation of the sand fraction not only provides a more complete description of the transport/bed surface interaction, but allows incorporation of a previously unmodeled nonlinear effect of sand content on gravel transport rates.

The model incorporates a hiding function that reduces the mobility of smaller sizes and increases the mobility of coarser sizes relative to the unisize case. The hiding function gives the variation of the reference shear stress (a surrogate for the critical shear

stress) as a function of fraction size relative to the median size of the bed surface. The function has two distinct limbs corresponding to relatively fine and relatively coarse fractions. Sandy sediments tend to have a relatively small median surface grain size, such that a majority of the fractions fall on the steep limb for coarser sizes. Sediments with little sand tend to have a relatively coarse median surface grain size, such that a majority of the fractions fall on the gentle limb for finer sizes. The two-part hiding function, combined with the influence of median surface size on the hiding function defined for individual sediments, provides an explanation for the apparent discrepancies among previously reported hiding functions.

Elements of the surface-based transport model developed here are similar to those of two previously defined models. The present model uses the full surface size distribution and is directly developed from a relatively comprehensive data set with an unambiguous measurement of surface grain size over a range of flow, transport rate, and sediment.

Acknowledgments

Experimental work was supported in part by the U.S. Department of Justice, Environment and Natural Resources Division, and by the U.S. Forest Service, Stream Systems Technology Center, Fort Collins, Colo., Stephen Kenworthy assisted in the laboratory; he and Brendan DeTemple provided valued feedback on model development. Comments from two anonymous reviewers helped us improve the paper.

Notation

The following symbols are used in this paper:

- D_i = grain size of fraction i ;
- D_{sm} = mean grain of bed surface;
- D_{50} = median grain size;

F_i = proportion of fraction i in surface size distribution;
 F_s = proportion of sand in surface size distribution;
 g = gravitational acceleration;
 P_i = proportion of fraction i in transport size distribution;
 q_b = transport rate per unit width;
 q_{bi} = transport rate of size fraction i per unit width;
 u_* = shear velocity;
 W_i^* = dimensionless transport rate of size fraction i [Eq. (2)];
 W_r^* = reference value of dimensionless transport rate (=0.002);
 $\phi = \tau/\tau_{ri}$;
 τ = shear stress;
 τ_{ci} = critical shear stress of size fraction i ;
 τ_r = reference shear stress;
 τ_{ri} = reference shear stress of size fraction i ;
 τ_{rm} = reference shear stress of mean size of bed surface;
 τ_i^* = dimensionless Shields stress for size fraction i ;
 τ_{rm}^* = reference dimensionless Shields stress for mean size of bed surface [Eq. (5)]; and
 ρ = water density.

References

- Andrews, E. D., and Erman, D. C. (1986). "Persistence in the size distribution of surficial bed material during an extreme snowmelt flood." *Water Resour. Res.*, 22, 191–197.
- Andrews, E. D., and Parker, G. (1987). "Formation of a coarse surface layer as the response to gravel mobility." *Sediment transport in gravel-bed rivers*, C. R. Thorne, J. C. Bathurst, and R. D. Hey, eds., Wiley, New York.
- Ashida, K., and Michue, M. (1971). "An investigation of river bed degradation downstream of a dam." *Proc., 14th Int. Association of Hydraulic Research Congress*, Vol. 3, Wallingford, U.K., 247–255.
- Ashworth, P. J., and Ferguson, R. I. (1989). "Size-selective entrainment of bed load in gravel bed streams." *Water Resour. Res.*, 25, 627–634.
- Chiew, Y-M., and Parker, G. (1994). "Incipient sediment motion on non-horizontal slopes." *J. Hydraul. Res.*, 32(5), 649–660.
- Church, M. A., McLean, D. G., and Wolcott, J. F. (1987). "River bed gravels: sampling and analysis." *Sediment transport in gravel-bed rivers*, C. R. Thorne, J. C. Bathurst, and R. D. Hey, eds., Wiley.
- Diplas, P., and Fripp, J. B. (1992). "Properties of various sediment sampling procedures." *J. Hydraul. Eng.*, 118(7), 955–970.
- Diplas, P., and Sutherland, A. J. (1988). "Sampling techniques for gravel sized sediments." *J. Hydraul. Eng.*, 114(5), 484–501.
- Egiazaroff, I. V. (1965). "Calculation of nonuniform sediment concentrations." *J. Hydraul. Div., Am. Soc. Civ. Eng.*, 91(4), 225–247.
- Einstein, H. A. (1950). "The bedload function for sediment transport in open channel flows." *Tech. Bull. No. 1026*, U.S. Dept. of Agriculture, Soil Conservation Service, Washington, D.C.
- Ettema, R. (1984). "Sampling armor-layer sediments." *J. Hydraul. Eng.*, 110(7), 992–996.
- Fripp, J. B., and Diplas, P. (1993). "Surface sampling in gravel streams." *J. Hydraul. Eng.*, 119(4), 473–490.
- Ikeda, H., and Iseya, F. (1988). "Experimental study of heterogeneous sediment transport." *Environmental Research Center Paper No. 12*, Univ. of Tsukuba, Japan.
- Jackson, W. L., and Beschta, R. L. (1984). "Influences of increased sand delivery on the morphology of sand and gravel channels." *Water Resour. Bull.*, 20(4), 527–533.
- Kellerhals, R., and Bray, D. I. (1971). "Sampling procedures for coarse alluvial sediments." *J. Hydraul. Div., Am. Soc. Civ. Eng.*, 97(8), 1165–1180.
- Kuhnle, R. A. (1989). "Bed-surface size changes in gravel-bed channel." *J. Hydraul. Eng.*, 115(6), 731–741.
- Kuhnle, R. A. (1993). "Incipient motion of sand-gravel sediment mixtures." *J. Hydraul. Eng.*, 119(12), 1400–1415.
- Marion, A., and Fraccarollo, L. (1997). "New conversion model for areal sampling of fluvial sediments." *J. Hydraul. Eng.*, 123(12), 1148–1151.
- Milhous, R. T. (1973). "Sediment transport in a gravel-bottomed stream." PhD thesis, Oregon State Univ., Corvallis, Ore.
- Paintal, A. S. (1971). "A stochastic model of bed load transport." *J. Hydraul. Res.*, 9(4), 527–554.
- Parker, G. (1990). "Surface-based bedload transport relation for gravel rivers." *J. Hydraul. Res.*, 28(4), 417–436.
- Parker, G., Dhamotharan, S., and Stefan, H. (1982a). "Model experiments on mobile, paved gravel bed streams." *Water Resour. Res.*, 18(5), 1395–1408.
- Parker, G., and Klingeman, P. C. (1982). "On why gravel bed streams are paved." *Water Resour. Res.*, 18, 1409–1423.
- Parker, G., Klingeman, P. C., and McLean, D. L. (1982b). "Bedload and size distribution in paved gravel-bed streams." *J. Hydraul. Div., Am. Soc. Civ. Eng.*, 108(4), 544–571.
- Parker, G., and Sutherland, A. J. (1990). "Fluvial Armor." *J. Hydraul. Res.*, 28(5), 529–544.
- Parker, G., and Wilcock, P. R. (1993). "Sediment feed and recirculating flumes: A fundamental difference." *J. Hydraul. Eng.*, 119(11), 1192–1204.
- Proffitt, G. T. (1980). "Selective transport and armoring of nonuniform alluvial sediments." *Rep. No. 80/22*, Dept. Civil Engineering, Univ. Canterbury, New Zealand, 203.
- Proffitt, G. T., and Sutherland, A. J. (1983). "Transport of nonuniform sediments." *J. Hydraul. Res.*, 21(1), 33–43.
- Rice, S., and Church, M. (1996). "Sampling surficial fluvial gravels: the precision of size distribution percentile estimates." *J. Sediment. Res.*, 66(3), 654–665.
- Sutherland, A. J. (1992). "Hiding functions to predict self-armoring." *Proc., Int. Association of Hydraulic, Research Int. Grain Sorting Seminar*, M. Jaeggi and R. Hunziker, eds., Mitteilungen der Versuchsanstalt für Wasserbau, Hydrologie und Glaziologie No. 117, ETH, Zurich, Switzerland.
- Vanoni, V. A., and Brooks, N. H. (1957). "Laboratory studies of the roughness and suspended load of alluvial streams." *Sedimentation Laboratory Rep. No. E68*, California Institute of Technology, Pasadena, Calif.
- Wilcock, P. R. (1988). "Methods for estimating the critical shear stress of individual fractions in mixed-size sediment." *Water Resour. Res.*, 24(7), 1127–1135.
- Wilcock, P. R. (1993). "Critical shear stress of natural sediments." *J. Hydraul. Eng.*, 119(4), 491–505.
- Wilcock, P. R. (1998). "Two-fraction model of initial sediment motion in gravel-bed rivers." *Science*, 280, 410–412.
- Wilcock, P. R. (2001). "The flow, the bed, and the transport: Interaction in flume and field." *Gravel-bed rivers V*, P. Mosley, ed., New Zealand Hydrological Society, Christchurch, N.Z., 183–219.
- Wilcock, P. R., and Kenworthy, S. T. (2002). "A two fraction model for the transport of sand/gravel mixtures." *Water Resour. Res.*, 38(10), 1194.
- Wilcock, P. R., Kenworthy, S. T., and Crowe, J. C. (2001). "Experimental study of the transport of mixed sand and gravel." *Water Resour. Res.*, 37(12), 3349–3358.
- Wilcock, P. R., and McArdell, B. W. (1993). "Surface-based fractional transport rates: Mobilization thresholds and partial transport of a sand-gravel sediment." *Water Resour. Res.*, 29(4), 1297–1312.
- Wilcock, P. R., and Southard, J. B. (1988). "Experimental study of incipient motion in mixed-size sediment." *Water Resour. Res.*, 24(7), 1137–1151.
- Wilcock, P. R., and Southard, J. B. (1989). "Bed-load transport of mixed-size sediment: Fractional transport rates, bed forms, and the development of a coarse bed-surface layer." *Water Resour. Res.*, 25, 1629–1641.
- Yalin, M. S. (1972). *Mechanics of sediment transport*, Pergamon, New York.